Electrical and structural properties of stepped, partially reconstructed Au(11*n*) surfaces in $HClO_4$ and H_2SO_4 electrolytes

Mohammad Alshakran[1], Guillermo Beltramo[1], Margret Giesen[1] and Harald Ibach[2*]

Institute for Bio- und Nano-Systems (1. IBN4, 2. IBN3), Jülich Forschungszentrum

D 52425 Jülich

Abstract

We have studied the interface capacitance and the voltammograms of Au(11*n*) (*n* = 5, 7, 11, 17) and of Au(100) electrodes in 5mM $HClO_4$ and 5mM H_2SO_4 after immersion into the electrolyte solution at –0.4V versus a saturated calomel electrode. The minima of the capacitance curves measured in positive sweeps continuously shift towards positive potentials as function of 1/*n*. All voltammograms, even that of Au(11 5), display peaks that are characteristic for lifting of surface reconstructions, albeit at different potentials. Thus, all vicinal surfaces appear to have at least sections that allow reconstruction. This inference is consistent with STM-profiles of an Au(11 9) surface which displays a wide range of local inclination angles corresponding to local (11 *n*)-orientations with $3.5 < n < \infty$. A numerical analysis of the voltammograms shows the existence of three different ranges of transition potentials for the lifting of the reconstruction. The transition potentials are assigned to three different structures of the reconstructed phase as either observed by experiment or proposed by theory.

* Corresponding author, e-mail: h.ibach@fz-juelich.de

1. Introduction

Clean Au(100) surfaces prepared either by heating in ultra-high vacuum or by flame-annealing in air are reconstructed. According to studies using X-ray diffraction [1, 2] the reconstruction consists of an incommensurate, nearly hexagonal densely-packed surface layer ("hex-layer"). The atom density in the hex-layer is about 25% higher than in the unreconstructed surface. Between 300K and 970K a coexistence of two phases is observed, one with the atom rows oriented exactly along a <110> direction, the other rotated by about 0.81° with respect to a <110>-direction. Above 970K only the aligned phase exists. STM studies show that at and near steps the reconstruction is always aligned exactly with the <110> orientation of kink-free steps [3, 4]. The observed coexistence of the aligned phase with the rotated phase is therefore to be attributed to the unavoidable presence of steps on nominally flat Au(100) surfaces.

The reconstruction can be lifted when the surface is in contact with an electrolyte and brought to potentials positive of the potential of zero charge (*pzc*) [5]. The effect was first observed in 1985 by Kolb and Schneider [6]. After lifting of the reconstruction the extra 25% atoms in the hex-layer (compared to the ideal (100) surface) assemble in islands on top of the original surface layer. Because of that, the Au(100) surface has been the preferred surface for studies of island shape fluctuations, island coalescence and Ostwald ripening in an electrolyte environment [7].

The lifting of the reconstruction is well understood as an equilibrium phenomenon [8-10]: For surfaces in contact with an electrolyte held at constant potential the surface tension contains a potential dependent term in addition to the Helmholtz free surface energy which for positive potential may outweigh the higher Helmholtz free surface energy of the unreconstructed phase (see also the discussion in sect. 4 of this paper).

While the lifting of the reconstruction occurs rather rapidly when the appropriate potential is reached [11], the reverse process is slow as the atoms need to dissociate from the islands and submerge into the first layer. The slowness of this activated reverse process enables the study of unreconstructed Au(100) surfaces in their metastable phase at lower potentials. The metastability has been exploited in the past to study the capacitance of the unreconstructed Au(100) surface and for the stepped Au(11*n*) surfaces for $5 \le n \le 17$. It has been shown that with increasing step density the *pzc* shifts to negative potentials due to the dipole moment associated with the steps [12]. Similar results have been obtained for Ag(11*n*) surfaces [13]. In all these cases the capacitance curves of Au(11*n*) in the unreconstructed state and Ag(11*n*) were rather alike and could well be explained by the shift in the *pzc* with increasing step density. A further, rather unexpected result was that the Helmholtz

capacitance of unreconstructed Au(11*n*) and Ag(11*n*) is substantially reduced compared to the Au(100) and Ag(100) surfaces, respectively [14].

The picture changes when stepped Au(11*n*) surface are immersed into the electrolyte at negative potential with respect to *pzc*. The *apparent pzc* as indicated by the minimum of the capacitance shifts drastically with the step density. The sharp peak in the voltammogram of a Au(100) that indicates the onset of the reconstruction (see e.g. Fig. 2.27 of [15]) is replaced by a complicated peak structure which, however, depends in a reproducible way on the step density and is qualitatively similar for different electrolytes. This paper shows that the challenging complicated appearance of the voltammograms and capacitance curves result from the inhomogeneity of the stepped Au(11*n*) crystal surfaces prepared by flame annealing in air or by heating in ultra-high vacuum in combination with different types of reconstruction on stepped surfaces. Height profiles of a nominal Au(119) surface investigated with scanning tunneling microscopy (STM) showed the presence of sections of a wide range of orientations from (113) to (100). A quantitative simulation of the voltammograms proves the existence of three different types of reconstruction characterized by a particular potential for the lifting of the reconstruction. Using a simple model the changes in the surface free energies involved in the reconstruction are calculated from the potentials for which the reconstruction is lifted. The three forms of the reconstruction are identified with the reconstruction on extended flat (100) terraces, the reconstruction on 5-25 nm terraces [4], and a reconstruction of smaller terraces which has been suggested theoretically [16].

2. Experimental

The experiments comprise electrical measurements (voltammograms and capacitance) as well as studies of the morphology using STM. For the electrical measurements we used bead-type single gold crystals, prepared by electron beam heating in ultra-high vacuum [17]. For the STM experiments crystals were cut from a single crystal rod. The crystals were oriented by diffractometry and polished to the desired orientation to within 0.1°, which is the accuracy of high-quality single crystals. The accuracy is naturally limited by the mosaic structure of the crystal. The bead crystals had (001)- and (11*n*)-orientations, with $n = 5$, 7, 11 and 17 corresponding to an angle θ with respect to the (100) plane where $\tan\theta = \sqrt{2}/n$ [7]. The crystal used in the STM study had (119) orientation. A geometrically ideal (11*n*) surface would consist of a train of equally spaced, monatomic high and parallel steps with (001)-oriented terraces in-between. The average terrace width is $L = na_{\perp}/2$ [7], with $a_{\perp}$ the distance between densely packed atomic rows (for Au(001) $a_{\perp} = 0.288$ nm).

Prior to experiments the single-crystal electrodes were flame-annealed to about 900 °C and cooled down to room temperature. Then, they were transferred to the cell under the protection of a droplet of deoxygenated water [18]. In order to investigate, whether the shapes of the voltammograms and capacitance curves depend on the sample preparation temperature, we performed also studies where the gold electrodes were annealed in a quartz-tube furnace with temperature control within ±2 °C. The annealing temperature was varied between 750 °C and 850 °C. Within the error margins, the voltammograms and capacitance curves were identical to those measured on flame-annealed samples. As electrolytes, we used suprapure $HClO_4$ and H_2SO_4 (Merck) and Milli-Q water (Millipore, 18.2 MΩ cm^{-1}). The electrical measurements were performed in 5mM $HClO_4$ and H_2SO_4. A saturated Hg/Hg_2SO_4 electrode in H_2SO_4 solution and a saturated calomel electrode (SCE) in $HClO_4$ served as reference electrodes. All potentials in this paper are therefore noted with respect to SCE. A platinum foil served as counter electrode. The surfaces were brought in contact with the electrolyte under potential control at –0.4V vs. SCE, hence well below *pzc*. Contact between the electrode surface and the solution was made by means of the hanging meniscus method. Cyclic voltammetry and capacitance curves were recorded using a Zahner IM5 impedance potentiostat.

The STM studies were performed in 10mM H_2SO_4. There, a platinum wire served as reference electrode. For further experimental details concerning the STM studies the reader is referred to reference [4].

3. Results

The results of the electrical measurements to be discussed in this paper are shown in Fig. 1 and Fig. 2. Fig. 1 shows the voltammograms and the capacitance curves of Au(11*n*) surfaces with *n*=5, 7, 11,and 17 as well as of the Au(100) surface for a 5mM $HClO_4$ electrolyte. Fig. 2 displays the same data for a 5mM H_2SO_4 electrolyte. In both cases the samples were immersed into the electrolyte under potential control immediately after the flame annealing procedures. All measurements were made during a positive potential sweep starting from the immersion potential of –0.4V. Thus, voltammograms and the capacitances were each measured with freshly prepared samples. The sweep rate in the voltammograms was 10mV/s. The capacitances are measured at 10mV intervals at a frequency of 20Hz with 5mV amplitude. We have also performed experiments where we used different frequencies (between 2 and 80 Hz) and different amplitudes (between 1 and 20 mV). In all these measurements, the capacitance curves exhibit merely minimal frequency dispersions

indicating that the double layer is almost perfectly described by a RC-equivalent circuit diagram, in accordance with observations by Eberhardt et al. [19].

In both electrolytes, the lifting of the reconstruction is indicated in the voltammograms of the Au(100) surface by the well-known peak at 0.37V in H_2SO_4 and at 0.6V in $HClO_4$. Lifting of the reconstruction results in a shift of the *pzc* and occurs beyond a particular potential when the surface tensions of the unreconstructed surface becomes lower than the surface tension of the reconstructed surface. The transition potential depends on the charge density and therefore on the type and concentration of the electrolyte. The transition potential is lower for H_2SO_4 because of the larger charge density due to specific adsorption of sulfate ions.

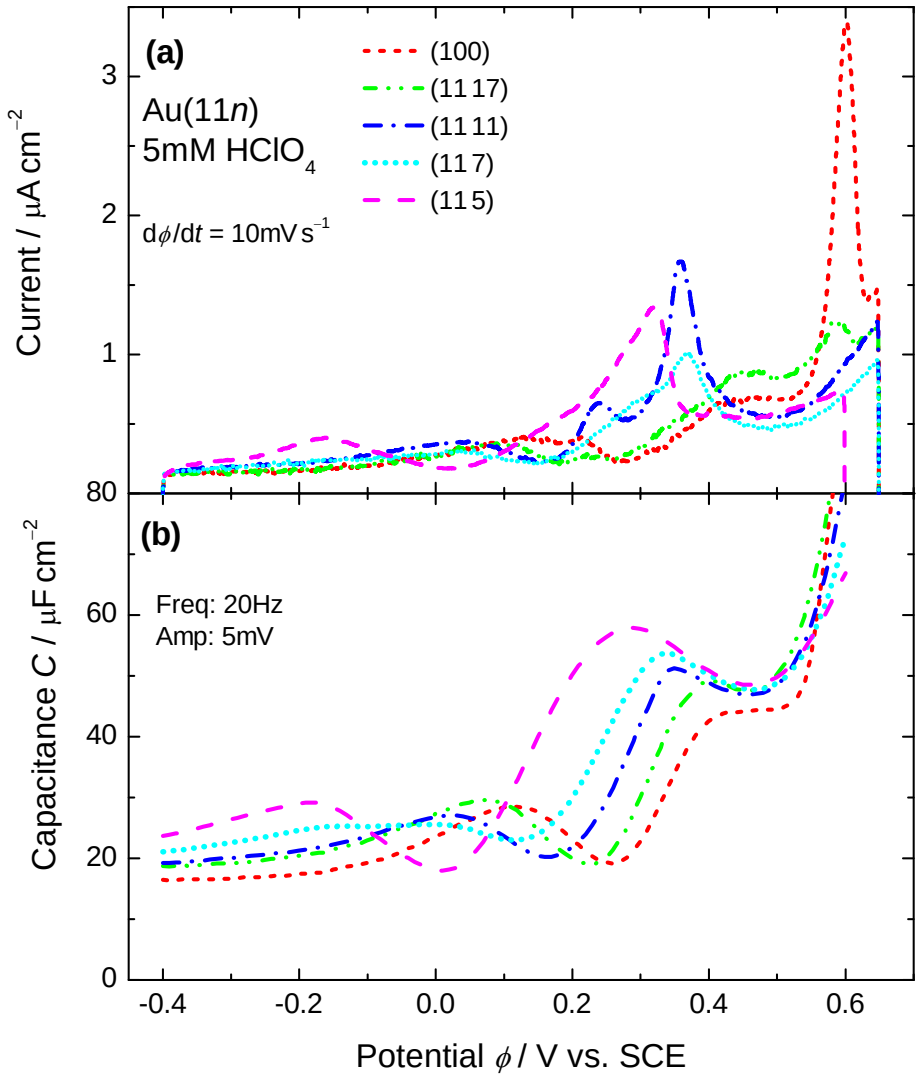

Fig. 1: (a) Voltammograms of Au(001) and Au(11*n*) (*n* = 5, 7, 11, and 17) in 5mM $HClO_4$ taken during a potential sweep starting from –0.4V immediately after immersing the samples into the electrolyte at –0.4 V so that the reconstructible sections of the surface are reconstructed. (b) Capacitance measured during the positive potential sweep.

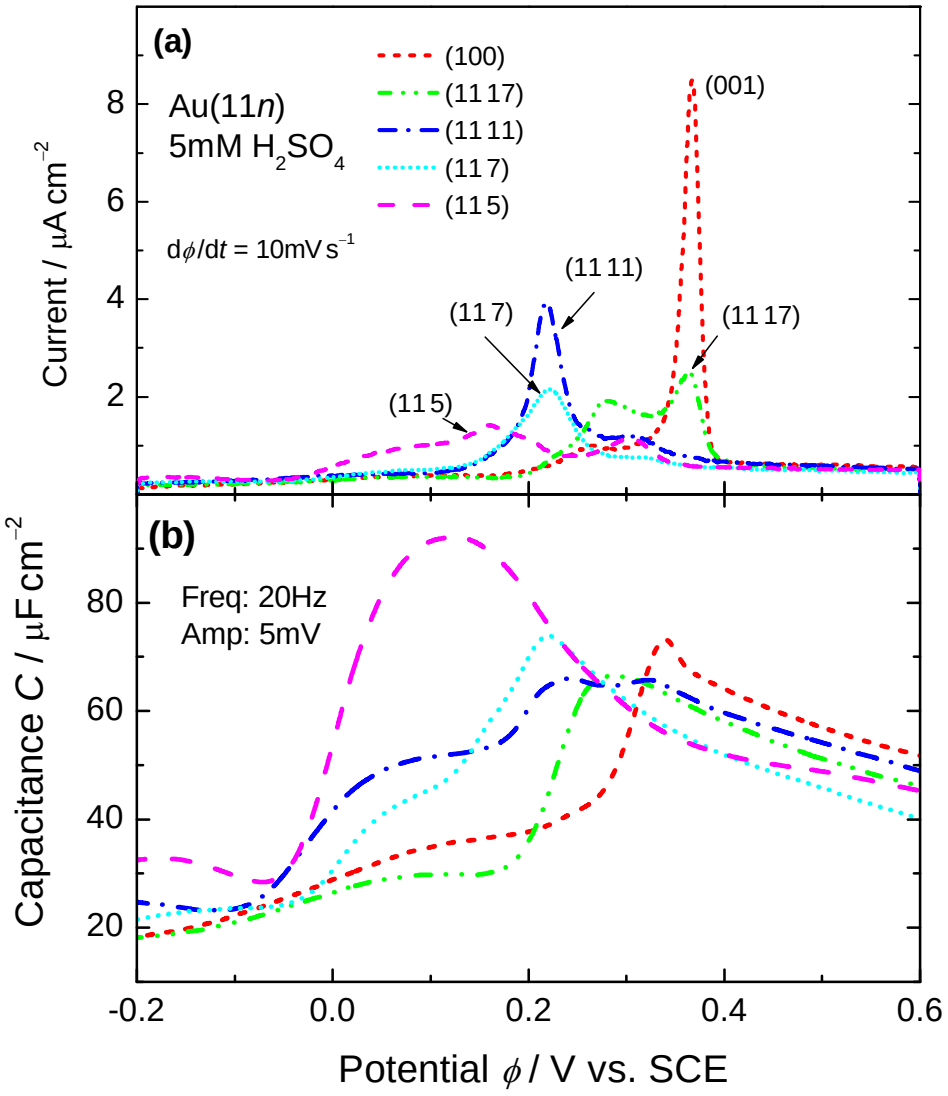

Fig. 2: (a) Voltammograms of Au(001) and Au(11*n*) (*n* = 5, 7, 11, and 17) in 5mM H_2SO_4 taken during a potential sweep starting from –0.35V vs. SCE immediately after immersing the samples into the electrolyte at –0.35 V vs. SCE so that the reconstructible sections of the surface are reconstructed. (b) Capacitance measured during the positive potential sweep.

In both electrolytes, the sharp transition peak for the Au(100) surface has a precursor, a shoulder around 0.42 V and 0.25 V for $HClO_4$ and H_2SO_4, respectively. This precursor shoulder on the Au(100) surface develops into a peak for the (11 17) surface. Vice versa, the main peak of the (100) surface reduces to a small peak on (11 17). A quantitative comparison of the capacitance curves and the voltammograms show that neither the precursor shoulder on the (100) surface nor the precursor peak on the (11 17) surface can be explained by the current required to load the capacitance. For example, the (11 17) surface in H_2SO_4 has a capacitance of 67 μF/cm^2 at 0.29 V (Fig. 2). With a scan speed of v=10mV/s one calculates a current

resulting from loading the capacitance of 0.67μA/cm^2. The measured current is 3 times as high however (1.8 μA/cm^2; Fig. 2). Hence, most of the current in that precursor must result from a lifting of a reconstruction and the shift in the *pzc* that comes with it. We are therefore lead to the conclusion that the (100) surface and the (11 17) surface possess two different transition potentials for lifting a reconstruction. Double peaks are also observed for the (11 11) and (11 7) surfaces. The details are different for the two electrolytes: For $HClO_4$, both surfaces display a small peak to be followed by the main peak, whereas for the H_2SO_4 electrolyte the main peak is followed by a smaller one. For the (115) sample finally one has a relatively broad peak preceded by a shoulder.

The capacitance curves in $HClO_4$ appear to be comparatively simple. Remarkable is the large shift in the minima from (115) to (100). Table 1 shows the position of the minima in the capacitance for positive potential sweeps in comparison to the minima for negative potential sweeps after the reconstruction was lifted. The latter data are taken from ref. [12].

Surface	$\vec{\phi}_{\min}$ / V	$\overleftarrow{\phi}_{\min}$ / V
Au(100)	0.257	0.041
Au(11 17)	0.226	0.027
Au(11 11)	0.164	0.019
Au(117)	0.115	0.008
Au(115)	0.009	-0.005

Table 1: Potentials of the minima in the capacitances curves for positive ($\vec{\phi}_{\min}$) and negative ($\overleftarrow{\phi}_{\min}$) sweeps in 5mM $HClO_4$ (Fig. 1b and [14]). For homogeneous surfaces the minima correspond to the potentials of zero charge (*pzc*). In a separate publication we show that for inhomogeneous surface as realized by Au(11*n*) the minimum marks the potential of zero mean charge on the surface [20].

A minimum in the capacitance is normally attributed to the minimum in the Gouy-Chapmann capacitance at *pzc*. The shift in the minima for negative sweeps is due to the increasing density of steps from (100) to (115) as the steps carry a dipole moment [12] which shifts the *pzc*. For the (100) surface where the step density is nominally zero the difference in the minima is due to the difference between the *pzc* of the reconstructed and the unreconstructed Au(100) surface. According to Table 1 the difference amounts to 0.216 V. This value is in agreement with earlier studies [9, 19]. The continuous shift in the minima in Fig. 1 from (115) to (100) is puzzling at first sight. According to ref. [4] the minimum terrace width required for

a "hex" reconstruction and a dead stripe around each step corresponds to the density of steps on a nominal (11 17) surface. Hence, neglecting the small shift due to the step dipole moments one would expect the capacitance minima in Fig. 1 to fall into two categories, one around 0V for the (11*n*) surfaces with $n < 17$, the other around 0.25V for $n \geq 17$. The peak structure in the voltammograms and the continuous shift indicate however that the surfaces with $n < 17$ are likewise at least partially reconstructed. The capacitance curves for the Au(11*n*) surfaces in H_2SO_4 (Fig. 2) show no well defined minima due to specific adsorption of sulfate ions starting at potentials below *pzc* [14].

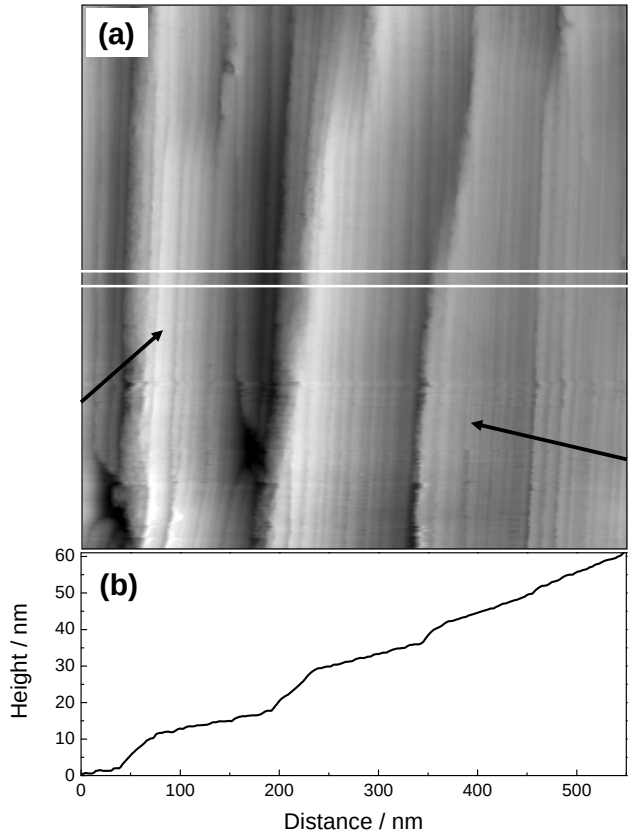

Fig. 3: (a) Typical STM image of an Au(119) surface prepared by flame annealing and studied in 10 mM H_2SO_4 electrolyte at -0.15V vs. SCE. Most of the "steps" seen in the image a small bunches of single monolayer high steps. The stripes between the steps are (100) terraces. Two examples are marked by arrows (b) Height profile of the STM-image averaged over the scan lines between the white lines in (a) after tilting the image plane such that (100) terraces are horizontal.

In order to elucidate the reason for the complexity of voltammograms and capacitance curve we have performed a systematic study of the morphology of an Au(119) surface using scanning tunneling microscopy (STM). A typical STM image of a surface prepared by flame annealing and studied in a 10mM H_2SO_4 electrolyte at –0.15V vs. SCE is shown in Fig. 3a. Whereas a typical copper or silver surface would display a more or less regular array of steps each one monolayer high [7], the image in Fig. 3 shows regions of steeper and smaller slopes.

Nearly all "steps" seen in the image are actually bunches of two or more steps of single atom height. While we cannot exclude the occasional formation of (111) microfacets consisting of two or three steps we have never observed extended (111) facets. This is consistent with earlier observations on Ag(19 19 17) surfaces [21]. Presumably the steps stay apart from each other because of repulsive step-step interactions [22, 23]. Close-up image furthermore show that the larger (100) terraces are reconstructed [4]. Fig. 3b shows a height profile obtained from the line-scans averaged between the white lines in Fig. 3a after tilting the image such that the (100) oriented terraces are horizontal. The profile as well as the image itself shows that the surface predominantly has regions with larger angles θ with respect to the (100) plane (tan $\theta \sim$ 0.25 - 0.3) and regions with smaller angles

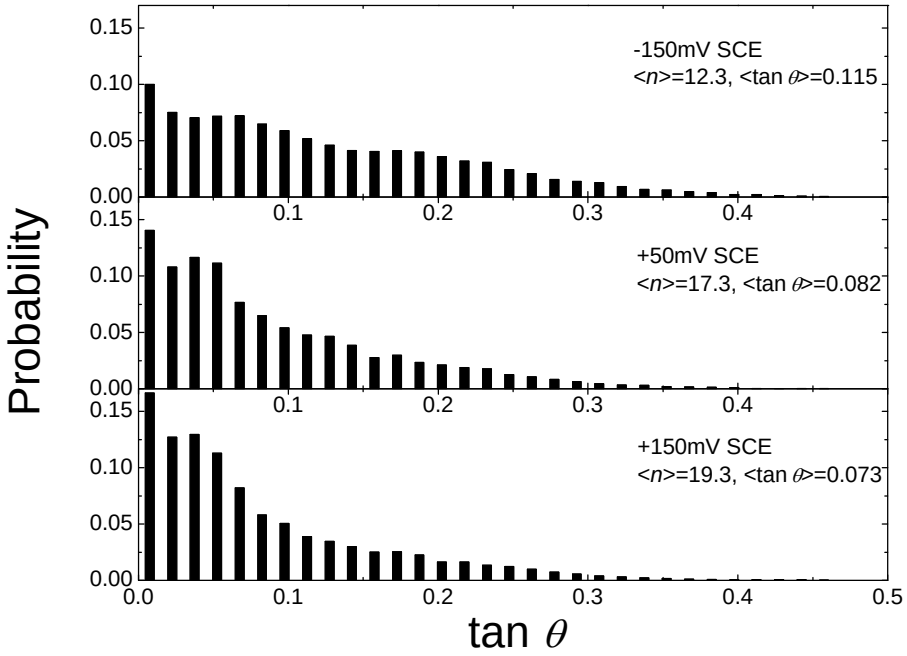

Fig. 4: Probability distributions to find a particular local orientation $\tan\theta$ at three different potentials. The distributions are obtained from line profiles as shown in Fig. 3 for 44 (-150mV), 44 (+50mV) and 32 (+150mV) images taken at different positions of the surface.

(tan $\theta \sim$ 0.05 - 0.15). This observation is consistent with our earlier findings for (119), (11 11) and (11 17) surfaces prepared by the same procedure as here [4].

In order to consider the relevance of the wide distribution of slopes for the area-averaging electrical properties we have performed a systematic study of the slopes in many (33-44) STM images taken at different positions of the surface and have determined the probability to find a particular angle of inclination with respect to the (100) plane. We have employed an algorithm which detects single steps and bunches of two and three steps. Surface sections that consist of a sequence of those events with intervening (100) terraces were assigned to a

common mean angle θ. Fig. 4 shows the histogram of the probabilities to find a particular $\tan\theta$ for electrode potentials of –0.15V, +0.05V, and +0.15V. We note that the mean $\tan\theta$ does not correspond to a (119) orientation for which $\langle\tan\theta\rangle$=0.157. This indicates that surface sections with steeper angles of inclination are omitted from the analysis. For example; (113) orientations with $\tan\theta = 0.47$ do not exist in the histograms. We have however occasionally also observed extended areas with angles of inclination that corresponded to (113) orientations. We have studied also individual surface ranges as function of time while the potential was held constant. In neither case we saw a change in the slope as function of time over time spans up to 30min. In view of this result the trend to smaller $\langle\tan\theta\rangle$ for larger potentials suggested by the histograms in Fig. 4 is considered to be an artifact.

A further issue of interest in the context of this study of the morphology of stepped surface is the fraction of the area consumed by (100) terraces that allow reconstruction. According to ref. [4] a minimum terrace width of 8.5 atom rows is required corresponding to $\tan\theta = 0.083$. About 50% of the (119) surface falls into that category. We finally have analyzed the surface morphology with regard to the mean width of the stripes that possess a common slope. Considering a slope as constant when it falls into a range $\Delta\tan\theta = \pm 0.0075$ (one bar in the histograms, Fig. 4) the mean structure size of sections with terrace sizes larger than 8.5 atom rows (n>17) was found to be around 10 nm. We did not find any indication of a "magic vicinal" (1 1 40) as observed in the phase diagram of a nominal Au(1 1 49) surface by Watson et al. [24]. This is not surprising, however. Because of the strong elastic repulsive interactions between steps one cannot expect the phase diagram of a particular orientation to be pertinent to orientations featuring a much higher step density.

The result of the STM studies may be summarized as follows: Au(11n) surfaces prepared by annealing to high temperatures show a wide distribution of local orientations due to a bunching of steps. The surface therefore consists of stripes of a mean width of 10 nm with grossly varying step density. This behavior is rather different from most other surfaces. In view of the fact that the key difference of gold surface is the reconstruction and since the reconstruction requires a minimum distance between steps, the energy reduction by reconstruction on (100) terraces is most likely the driving force for the step bunching instability of Au(11n) surfaces. We note that there is no preference for particular orientations. While this experimental fact is consistent with our earlier study [4], it is, however, at variance with a theoretical prediction of Bartolini et al. who found a particular stability of (11 11) and (115) surfaces.

4. Discussion of voltammograms

This section focuses on the discussion of the surprisingly complicated peak structure of the voltammograms as displayed in Fig. 1a and 2a. The discussion of the capacitance of the partially reconstructed surfaces requires a complex analysis of the capacitance of surfaces with inhomogeneous *pzc*s employing a numerical solution of the Poisson Boltzmann equation. This will be presented in separate paper [20]. Here, we merely quote from that study that the capacitance of a surface with inhomogeneous *pzc*s is approximately equal to the capacitance of a surface with a single mean *pzc* as long as the characteristic size of the structure is not larger than about 3 times the Debye length of the electrolyte (here $d_{\mathrm{Debye}} = 4\mathrm{nm}$). The minimum in the capacitance is then at the potential of zero mean charge (*pzmc*).

By way of introduction to the discussion of the voltammograms we first reiterate the well-documented interpretation of the lifting of the reconstruction and its effect on the voltammogram for the flat (100) surface. For both electrolytes, the peak in the voltammograms of Au(100) is attributed to the lifting of the hex-reconstruction (see e.g. [15], p. 99). Due to the lower *pzc* of the unreconstructed surface (Table 1) a sudden lifting of the reconstruction is accompanied by a change in the surface charge density and thus by a current burst in the voltammogram. The reason for the lifting of the reconstruction is the fact the surface tension γ of the unreconstructed surface becomes lower than the surface tension of the reconstructed surface beyond a particular potential [8, 9]. This is illustrated in Fig. 5.

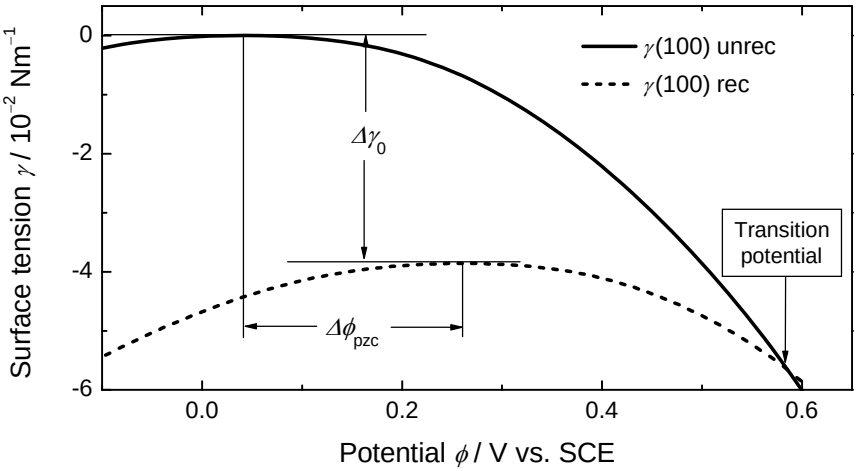

Fig. 5: Surface tension of the unreconstructed and the reconstructed Au(100) surface in 5mM $HClO_4$ (solid and dashed lines, respectively). The two curves are displaced on the vertical axis with respect to each other by $\Delta\gamma_0$ to match the transition potential to the experiment. The difference $\Delta\gamma_0$ is the difference in the Helmholtz free energies of the two surfaces, in other words, the gain in free energy due to reconstruction.

The dashed and solid lines in Fig. 5 represent the surface tensions of the reconstructed and unreconstructed Au(100) surfaces in 5mM $HClO_4$. The shape of the surface tension curves are calculated using (see e.g. [15], p.162)

$$\gamma(\phi) = \gamma_{\mathrm{pzc}} + \int_{\phi_{\mathrm{pzc}}}^{\phi} \sigma(\tilde{\phi})\mathrm{d}\tilde{\phi}, \qquad \sigma(\phi) = \int_{\phi_{\mathrm{pzc}}}^{\phi} C(\tilde{\phi})\mathrm{d}\tilde{\phi} \tag{1}$$

in which $\sigma(\phi)$ is the surface charge density, $C(\phi)$ the area-specific capacitance, ϕ_{pzc} the potential of zero charge (*pzc*), and γ_{pzc} is the surface tension at *pzc*, i.e. the specific Helmholtz free energy of the surface [15]. For the reconstructed surface γ_{pzc} is arbitrarily set to zero; for the unreconstructed surface γ_{pzc} is set to $-3.9\ 10^{-2}$ N/m in order to match the transition potential in Fig. 5 to the experimentally observed transition potential. The displacement of the $\Delta\gamma$ for the two surfaces corresponds to the gain in the free energy due to the reconstruction. The value $\gamma_{\mathrm{pzc}} = -0.039$ N/m obtained here agrees with an earlier result of Santos and Schmickler within the quoted error bars in ref. [9]. It is furthermore consistent with a recent theoretical study by Feng et al. [10]. A similar value of γ_{pzc} is obtained for the H_2SO_4 electrolyte if one assumes the same *pzc* as for $HClO_4$. However, the exact value for the *pzc* cannot be obtained from experiment in that case since the capacitance for the reconstructed Au(100) surface does not show a clear minimum due to the specific adsorption of sulfate. From the shape of the capacitance curve one estimates the *pzc* of the reconstructed Au(100) surface in H_2SO_4 to be also between 0.25 and 0.26V vs. SCE.

The voltammograms of the stepped Au(11*n*) surfaces display likewise peaks that are to be attributed to a lifting of reconstruction. The fact that the voltammograms in $HClO_4$ and H_2SO_4 are rather similar except for the compression into a smaller potential range for the H_2SO_4 electrolyte proves that the voltammograms result from genuine properties of the stepped gold surfaces. The broad distribution of the slopes on stepped surfaces (Fig. 4) leaves room for sections with distances between steps large enough to allow for reconstructions. In an earlier STM study on nominal (119), (11 11) and (11 17) surfaces reconstructed terraces of 5-25 nm width were observed [4]. The reconstruction on these terraces differs from the reconstruction on flat surfaces in several ways: the <110> aligned reconstruction lines have a periodicity that is significantly enlarged compared to flat (100) surfaces. There is furthermore an unreconstructed stripe of 2-4 atom rows along each step. The voltammograms of the (11 17) surface in Fig. 1 and 2 show two peaks, one approximately at the potential where the reconstruction of the flat (100) surface is lifted, and one at a smaller potential. The former one

is obviously associated with the lifting of the reconstruction on extended (100) terraces on the nominal (11 17) surface while the latter is presumably attributed to lifting of the different reconstruction observed on the 5-25 nm wide terraces. From the smaller transition potential one can infer that the reduction of the surface tension $\Delta\gamma_0$ due to this type of reconstruction is smaller than on flat Au(100).

The (11 17) is not the only surface for which the voltammogram displays two peaks. Two peaks or a peak and a shoulder are actually observed for all (11*n*) surfaces. Particular surprising is the occurrence of reconstruction peaks in the voltammograms of Au(115) on which one would have expected that merely a small fraction of the surface possesses terraces large enough for reconstruction.

5. Quantitative analysis of the voltammograms

In order to elucidate the reason for the complex voltammograms we calculate the voltammograms from the capacitances of the reconstructed and unreconstructed surfaces in the following. The method is first outlined for a single type of reconstruction. The extension to two or more different types with different transition potentials is then straightforward. By definition the current density in the voltammogram is

$$j(\phi) = v\frac{\mathrm{d}}{\mathrm{d}t}C(\phi) = v\frac{\mathrm{d}}{\mathrm{d}t}\left(\kappa_{\mathrm{rec}}(\phi)C_{\mathrm{rec}}(\phi) + \kappa_{\mathrm{unrec}}(\phi)C_{\mathrm{unrec}}(\phi)\right). \qquad (2)$$

Here, $v = \mathrm{d}\phi/\mathrm{d}t$ is rate by which the potential is changed in recording the voltammogram and κ_{rec} and κ_{unrec} are the fractions of the surface area A that bear the capacitance C_{rec} and C_{unrec}, respectively

$$\kappa_{\mathrm{rec}} = A_{C_{\mathrm{rec}}} / A,\ \kappa_{\mathrm{unrec}} = A_{C_{\mathrm{unrec}}} / A. \qquad (3)$$

Note that on stepped surfaces the area $A_{C_{\mathrm{rec}}}$ does include areas where the step density is too high to permit reconstruction just as C_{rec} is the measured capacitance of a surface that includes areas that cannot reconstruct because of the high step density. Therefore by definition one has

$$\kappa_{\mathrm{rec}} = 1 - \kappa_{\mathrm{unrec}} \qquad (4)$$

We note further that

$$\kappa_{\mathrm{rec}} = 1, \;\; \phi < \phi_{\mathrm{t}} \tag{5}$$

where ϕ_{t} is the transition potential beyond which the reconstruction is lifted.

We have tried several forms for an ansatz for the growth of the fraction of the unreconstructed areas as function of the potential ϕ. Good fits to the experimental voltammograms were obtained by assuming the transition does not require a critical nucleus but rather follows directly the driving force which is the difference in the surface tensions of the reconstructed and the unreconstructed surface. This difference is linear to lowest order in the potential and quadratic to next higher order. Hence we make the ansatz

$$\frac{\mathrm{d}\kappa_{\mathrm{rec}}}{\mathrm{d}t} = -\alpha(\phi - \phi_{\mathrm{t}})^{\beta}\,\Theta(\phi - \phi_{\mathrm{t}})\,\kappa_{\mathrm{rec}} \tag{6}$$

with $\beta = 1,\ 2$ and $\Theta(\phi - \phi_{\mathrm{t}})$ the Heavyside function ($\Theta(\phi - \phi_{\mathrm{t}}) = 0$ for $\phi \le \phi_{\mathrm{t}}$; $\Theta(\phi - \phi_{\mathrm{t}}) = 1$ for $\phi > \phi_{\mathrm{t}}$). The rate constant α is a fitting parameter describing the kinetics of the transition. The proportionality to κ_{rec} implies that the lifting of the reconstruction can occur anywhere on the reconstructed area. STM images of the Au(100) surface in which the potential was changed between one scan line and the next show that this is indeed the case [11]. For a constant velocity in the change of the potential $v = \mathrm{d}\phi/\mathrm{d}t$, as used in the recording of voltammogram, the time in eq. 6 can be integrated out and one obtains

$$\kappa_{\mathrm{rec}}(\phi) = \exp\!\left(-\frac{\alpha}{2v}(\phi - \phi_{\mathrm{t}})^2\,\Theta(\phi - \phi_{\mathrm{t}})\right), \;\; \beta = 1 \tag{7}$$

$$\kappa_{\mathrm{rec}}(\phi) = \exp\!\left\{-\frac{\alpha}{2v}\left((\phi^3 - \phi_{\mathrm{t}}^3)/3 - \phi^2\phi_{\mathrm{t}} + \phi_{\mathrm{t}}^2\phi\right)\Theta(\phi - \phi_{\mathrm{t}})\right\}, \;\; \beta = 2 \tag{8}$$

The current density then becomes

$$\begin{aligned} j = {} & v\left(\kappa_{\mathrm{rec}}(\phi)C_{\mathrm{rec}}(\phi) + (1 - \kappa_{\mathrm{rec}})C_{\mathrm{unrec}}(\phi)\right) \\ & + \alpha(\phi - \phi_{\mathrm{t}})^{\beta}\,\Theta(\phi - \phi_{\mathrm{t}})\kappa_{\mathrm{rec}}\left(\sigma_{\mathrm{rec}}(\phi) - \sigma_{\mathrm{unrec}}(\phi)\right) \end{aligned} \tag{9}$$

Here, $\sigma_{rec}(\phi)$ and $\sigma_{unrec}(\phi)$ are the surface charge densities averaged over the sample for each potential since the experimentally measured current densities are likewise an average over the surface and thus corresponds to variations in the average charge densities. The charge densities $\sigma_{rec}(\phi)$ and $\sigma_{unrec}(\phi)$ can be calculated from the measured capacitances $C_{rec}(\phi)$ and $C_{unrec}(\phi)$ provided one knows the potential where the average charge density on the surface is zero. As remarked before we will show in a separate paper [20] that this potential of zero mean charge is nearly at the minimum of the capacitance as long as the mean structure size does not exceed the Debye-length by more than a factor of three.

Eq. 9 can be generalized to allow for two differently reconstructed surface sections with fractional areas f_1 and f_2 ($f_1+f_2 = 1$) with different transition potentials ϕ_{t1} and ϕ_{t2}.

$$\begin{aligned} j = \nu\{&\big(f_1\kappa_{rec1}(\phi) + f_2\kappa_{rec2}(\phi)\big)C_{rec}(\phi) + \big(1-\kappa_{rec1}(\phi)-\kappa_{rec2}(\phi)\big)C_{unrec}(\phi)\} \\ &+ \Big\{\alpha_1(\phi-\phi_{t1})^{\beta}\Theta(\phi-\phi_{t1})\,f_1\kappa_{rec1}(\phi) + \alpha_2(\phi-\phi_{t2})^{\beta}\Theta(\phi-\phi_{t2})\,f_2\kappa_{rec2}(\phi)\Big\} \\ &\times\big(\sigma_{rec}(\phi)-\sigma_{unrec}(\phi)\big) \end{aligned} \qquad (10)$$

In writing eq. 10 we make use of the fact that the measured capacitance $C_{rec}(\phi)$ between ϕ_{t1} and ϕ_{t2} is the capacitance of a surface for which one type of the reconstruction is already lifted at the potential ϕ_{t1}. Hence the charge burst after the second transition potential ϕ_{t2} is correctly described, provided that the *pzc*s of the differently reconstructed areas are the same. As the two reconstructions considered above involve nearly the same atom density in the surface layer the assumption of the same *pcz* may be justified.

Using eq. 10 we have simulated the voltammograms for the $HClO_4$ electrolyte with the help of the experimental capacitance data for $C_{rec}(\phi)$ (Fig. 1) and $C_{unrec}(\phi)$ from [14]. A slightly better fit was obtained with the ansatz $\beta = 2$ (eq. 8). The optimum fits for $\beta = 2$ are shown in Fig. 6. The relevant fitting parameters are listed in Table 2. A very similar set of parameters is obtained by fitting with the ansatz with $\beta = 1$. This set of parameters is listed in Table 3.

The results show that the transition potentials fall into three categories, one around $\phi_{t1} = 0.56$V (0.58V), one at about $\langle\phi_{t2}\rangle = 0.30\pm0.02$V (0.33±0.04V) and finally one which occurs only on surfaces with a very high step density at about $\langle\phi_{t3}\rangle = 0.13\pm0.02$V (0.17±0.02V). The numbers in brackets denote the results for the model with $\beta = 1$ (Table 3).

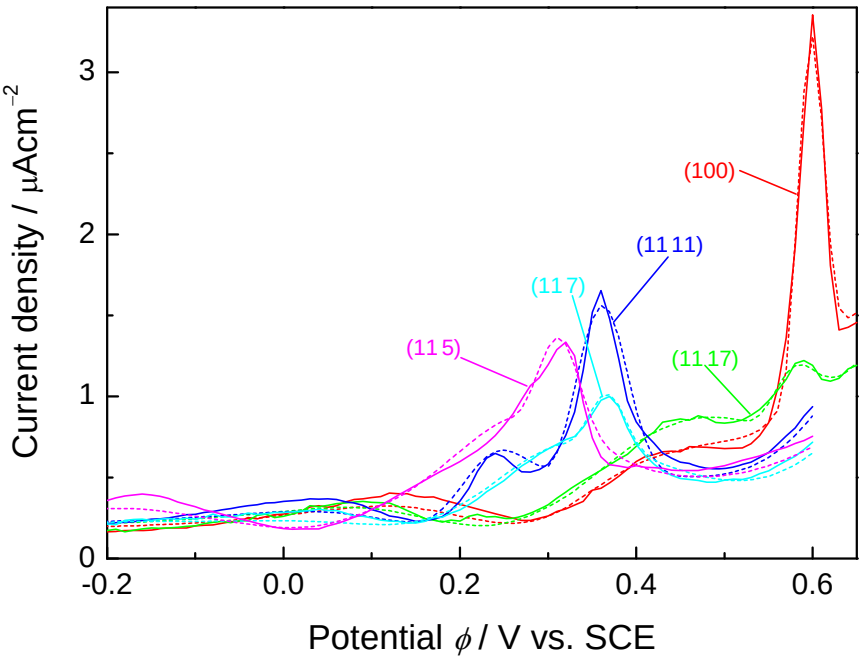

Fig. 6: Voltammograms of Au(100) and Au(11*n*) surface with $n = 5, 7, 11, 17$ in 5mM $HClO_4$. Solid lines are the experimental data from Fig. 1, dashed lines the calculations for $\beta = 2$ using five parameters, the rates α_1 and α_2, the transition potentials ϕ_{t1} and ϕ_{t2} and f_1 the area fraction for reconstruction of type 1. The resulting parameters of interest are listed in Table 2.

surface	f_1	ϕ_{t1}/V	$\Delta\gamma_1$/0.01N/m	f_2	ϕ_{t2}/V	$\Delta\gamma_2$/0.01N/m	f_3	ϕ_{t3}/V	$\Delta\gamma_3$/0.01N/m
(100)	0.58	0.56	-3.9	0.42	0.29	-1.0			
(11 17)	0.22	0.53	-3.0	0.78	0.31	-1.3			
(11 11)				0.68	0.30	-1.3	0.32	0.15	-0.23
(117)				0.22	0.32	-1.5	0.78	0.12	-0.16
(115)				0.23	0.26	-1.1	0.62	0.12	-0.24

Table 2: Fitting parameters for the best fits to the voltammograms for $\beta = 2$. Note that the transition potentials ϕ_{ti} mark the onset of the lifting of the respective reconstructions, not the peaks in the voltammograms! The positions of the peaks depend on the transition potentials, but to a lesser extent also on the rate constants α_i. The values for $\Delta\gamma_i$ are obtained from the required downshift of the surface tension of the reconstructed surface to obtain the transition potentials ϕ_{ti} (see text for discussion).

surface	f_1	ϕ_{t1}/V	$\Delta\gamma_1$/0.01N/m	f_2	ϕ_{t2}/V	$\Delta\gamma_2$/0.01N/m	f_3	ϕ_{t3}/V	$\Delta\gamma_3$/0.01N/m
(100)	0.52	0.58	–4.0	0.48	0.36	–1.7			
(11 17)	0.20	0.54	–3.0	0.80	0.36	–1.7			
(11 11)				0.67	0.32	–1.5	0.33	0.17	–0.36
(117)				0.24	0.34	–1.5	0.76	0.19	–0.45
(115)				0.47	0.27	–1.1	0.53	0.14	–0.32

Table 3: Fitting parameters for the best fits to the voltammograms for $\beta = 1$. The values for $\Delta\gamma_i$ are obtained from the required downshift of the surface tension of the reconstructed surface to obtain the transition potentials ϕ_{ti} (see text for discussion).

The transition potentials ϕ_{t1} and ϕ_{t2} are obviously associated with the lifting of the reconstruction of extended (100) surfaces and the particular reconstruction occurring on the 5-25 nm wide terraces of stepped surfaces, respectively. The results show that the latter type of reconstruction occurs on all Au(11*n*) surfaces, however with a smaller weight with respect to the competing reconstruction on surfaces with smaller *n*. Surprisingly, this reconstruction occurs also on the nominally flat (100) surface. This means that a comparatively small concentration of steps can change the mode of reconstruction in parts of the surface. The third transition potential ϕ_{t3} could be associated with a hitherto experimentally not identified type of reconstruction. This reconstruction presumably occurs on surface sections where the step density is too high to accommodate the hex-reconstruction plus an unreconstructed stripe next to steps. Theoretically, the various reconstructions on Au(11*n*) surfaces were studied by Bartolini et al. [16] employing a many body model potential. The authors found a reconstruction on the terraces of a (11 11) surface with 11.7% extra atoms in the surface layer. According to their calculations the (11 11) surface should be particular stable and a nominal (11 11) surface should therefore display a regular array of steps and terraces. While this proposition is not supported by our studies the calculations show at least that reconstructions with additional atoms in the surface may be possible even on narrow terraces.

The two transition potentials ϕ_{t2} and ϕ_{t3} associated with stepped regions of the surface are smaller than the transition potential ϕ_{t1} for the flat (100) surfaces. According to the construction shown in Fig. 5 the lower transition potentials indicate a smaller downshift of the surface tension curve of the reconstructed surface compared to the (100) case, hence a smaller gain in the Helmholtz free energy due to reconstruction. To turn this argument into a quantitative statement one would need the potential dependence of the surface tension of the particular stepped regions for which the reconstruction is being considered. However, only the mean capacitance and the mean *pzc* of the partially reconstructed stepped surface and therefore the potential dependence of the mean surface tension is known from experiment (Fig. 1b). In order to estimate the gain in the Helmholtz free energy for the reconstructions on the stepped surfaces we make the assumption that the potential dependence of the local surface tension is the same as for the mean surface tension so that only the Helmholtz free energies γ_{i0} depend on the type of reconstruction. It is shown in ref. [20] that the assumption is justified for the 5mM electrolyte concentration and the mean structure size of 10nm. Hence, we write

$$\gamma_i^{(\mathrm{rec})}(\phi) = \gamma_{i0}^{(\mathrm{rec})} + \left\langle \gamma^{(\mathrm{rec})}(\phi) \right\rangle \tag{11}$$

and

$$\gamma_i^{(\mathrm{unrec})}(\phi) = \gamma_{i0}^{(\mathrm{unrec})} + \left\langle \gamma^{(\mathrm{unrec})}(\phi) \right\rangle . \tag{12}$$

The transition potential is defined by

$$\gamma_i^{(\mathrm{rec})}(\phi_\mathrm{t}) = \gamma_i^{(\mathrm{unrec})}(\phi_\mathrm{t}) , \tag{13}$$

so that the difference of the Helmholtz free energy is

$$\Delta\gamma_i \equiv \gamma_{i0}^{(\mathrm{rec})} - \gamma_{i0}^{(\mathrm{unrec})} = \left\langle \gamma^{(\mathrm{unrec})}(\phi_{\mathrm{t}i}) \right\rangle - \left\langle \gamma^{(\mathrm{rec})}(\phi_{\mathrm{t}i}) \right\rangle$$

The resulting individual values for the $\Delta\gamma_i$ are listed in Tables 2 and 3. For the reconstruction on the (100) surface the best values for $\Delta\gamma$ are $-3.9\ 10^{-2}$N/m and $-4\ 10^{-2}$N/m for $\beta = 2$ and $\beta = 1$, respectively. For the reconstruction on wider terraces the mean values are $\Delta\gamma_2 = 1.2\pm0.2\ 10^{-2}$N/m and $\Delta\gamma_2 = 1.5\pm0.3\ 10^{-2}$N/m for $\beta = 2$ and $\beta = 1$, respectively. For the third type of reconstruction finally one obtains the mean values $\Delta\gamma_3 = 0.20\pm0.04\ 10^{-2}$N/m and $\Delta\gamma_3 = 0.37\pm0.07\ 10^{-2}$N/m. As expected from the transition potentials, the energy gains $\Delta\gamma_i$ for the reconstructions on the stepped sections of the surface are significantly lower compared to the energy gain for the reconstruction on the flat (100) surface. The accuracy of the values is difficult to assess, however.

6. Variation of the voltammograms with the scan speed

While the shape of the voltammograms primarily depend on the transition potentials $\phi_{\mathrm{t}i}$ the exact position of the peaks in the voltammograms are also affected by the kinetic parameters α in eq. 6. These parameters α are fixed by the optimum simulation of the experimental data. Once a kinetic parameter is fixed for a particular surface it describes also the variation of a peak position in the voltammogram with the scan speed. In order to add to the credibility of our modeling we have studied the shift in the position of the main peaks on Au(100) and Au(11 11), both in experiment and in the simulations for scan speed between 10mV/s and 500mV/s.. As the peaks shift to positive potentials with increasing scan speed the

voltammograms in $HClO_4$ would carry the surface into the range of oxide formation for high scan speeds. We have therefore studied the peak shifts in 5mM H_2SO_4. For the *pzc*s of the reconstructed and unreconstructed surfaces we assume the values determined for the $HClO_4$ electrolyte. This assumption is not critical as the position of the peak is rather insensitive to the *pzc*s.

Fig. 7 shows the experimentally observed positions of the maxima in the voltammograms as function of the scan speed for Au(100) and Au(11 11) as circles and squares, respectively. The solid line and dashed lines represents the peak positions obtained from the simulations for $\beta = 2$ and with all parameters kept fixed to the values obtained for the optimum fit to the scan speed 10mV/s. The experimentally data match rather nicely to the simulations. Our model therefore describes the kinetics of the lifting of the reconstruction correctly.

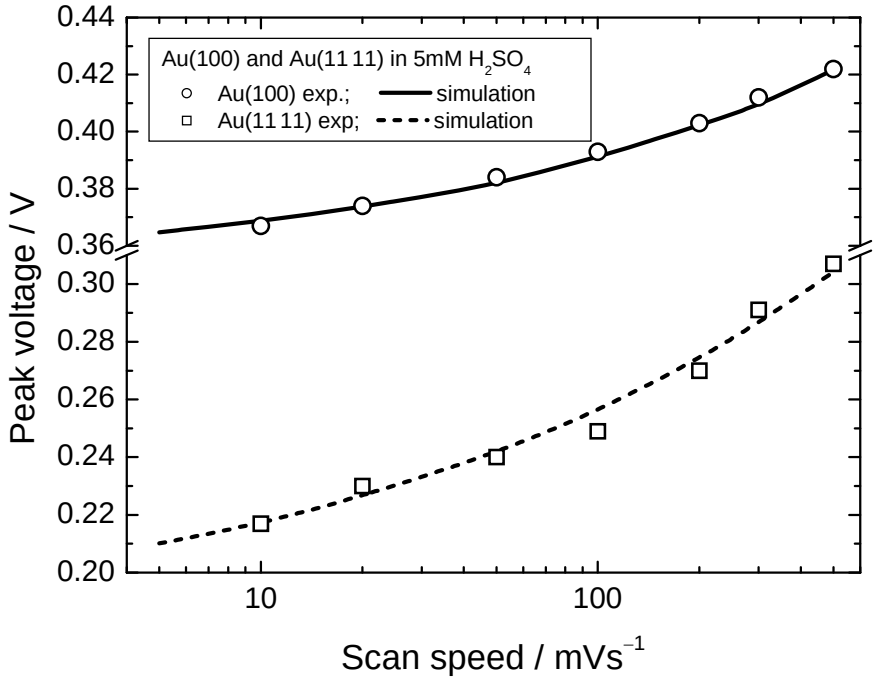

Fig. 7: Voltage of the peaks in the voltammograms as function of the scan speed. Experimental peak positions for Au(100) and Au(11 11) are shown as circles and squares, respectively. The solid and dashed lines are the results of the simulations.

7. Conclusions

Au(11*n*) surfaces display an extremely wide terrace width distribution. The complex, yet reproducible voltammograms of these surfaces can be explained quantitatively by a model that involves three different types of reconstructions. By comparison to previous studies two

of them can be identified as the reconstructions on extended flat (100) terraces and on 5-25 nm wide terraces, respectively. The analysis of the data using a simplifying model shows that the gain in surface free energy due to reconstruction for the latter type of reconstruction is less than one half of the gain on the flat Au(100) surface. The third type of reconstruction is associated with terraces that are too small to accommodate the normal hex-reconstruction and a reconstruction free zone at the steps. Here, the gain in surface energy is even smaller.

References

[1] S. G. J. Mochrie, D. M. Zehner, B. M. Ocko, D. Gibbs, Phys. Rev. Lett. 64 (1990) 2925.
[2] B. M. Ocko, D. Gibbs, K. G. Huang, D. M. Zehner, S. G. J. Mochrie, Phys. Rev. B 44 (1991) 6429.
[3] C. Bombis, H. Ibach, Surf. Sci. 564 (2004) 201.
[4] M. Moiseeva, E. Pichardo-Pedrero, G. Beltramo, H. Ibach, M. Giesen, Surf. Sci. 603 (2009) 670.
[5] D. M. Kolb, Prog. Surf. Sci. 51 (1996) 109.
[6] D. M. Kolb, J. Schneider, Surf. Sci. 162 (1985) 764.
[7] M. Giesen, Prog. Surf. Sci. 68 (2001) 1.
[8] H. Ibach, E. Santos, W. Schmickler, Surf. Sci. 540 (2003) 504.
[9] E. Santos, W. Schmickler, Chem. Phys. Lett. 400 (2004) 26.
[10] Y. J. Feng, K. P. Bohnen, C. T. Chan, Phys. Rev. B 72 (2005) 125401.
[11] A. S. Dakkouri, Solid State Ionics 94 (1997) 99.
[12] G. L. Beltramo, H. Ibach, M. Giesen, Surf. Sci. 601 (2007) 1876.
[13] G. Beltramo, H. Ibach, U. Linke, M. Giesen, Electrochim. Acta 53 (2008) 6818.
[14] G. Beltramo, M. Giesen, H. Ibach, Electrochim. Acta 54 (2009) 4305.
[15] H. Ibach, *Physics of Surfaces and Interfaces*, Springer, Berlin, Heidelberg, New York 2006.
[16] A. Bartolini, F. Ercolessi, E. Tosatti, Phys. Rev. Lett. 63 (1989) 872.
[17] B. Voigtländer, U. Linke, H. Stollwerk, J. Brona, J. Vac. Sci. Technol. A 23 (2005) 1535.
[18] A. Hamelin, J. Electroanal. Chem. 386 (1995) 1.
[19] D. Eberhardt, E. Santos, W. Schmickler, J. Electroanal. Chem. 419 (1996) 23.
[20] G. Beltramo, M. Giesen, H. Ibach, to be published.
[21] S. Baier, H. Ibach, M. Giesen, Surf. Sci. 573 (2004) 17.
[22] M. E. Fisher, D. S. Fisher, Phys. Rev. B 25 (1982) 3192.
[23] N. C. Bartelt, T. L. Einstein, E. D. Williams, Surf. Sci. 240 (1990) L591.
[24] G. M. Watson, D. Gibbs, D. M. Zehner, M. Yoon, S. G. J. Mochrie, Surf. Sci. 407 (1998) 59.